

Robustness in simple biochemical networks

N. Barkai & S. Leibler

Departments of Physics and Molecular Biology, Princeton University, Princeton, New Jersey 08544, USA

Cells use complex networks of interacting molecular components to transfer and process information. These “computational devices of living cells”¹ are responsible for many important cellular processes, including cell-cycle regulation and signal transduction. Here we address the issue of the sensitivity of the networks to variations in their biochemical parameters. We propose a mechanism for robust adaptation in simple signal transduction networks. We show that this mechanism applies in particular to bacterial chemotaxis²⁻⁷. This is demonstrated within a quantitative model which explains, in a unified way, many aspects of chemotaxis, including proper responses to chemical gradients⁸⁻¹². The adaptation property^{10,13-16} is a consequence of the network’s connectivity and does not require the ‘fine-tuning’ of parameters. We argue that the key properties of biochemical networks should be robust in order to ensure their proper functioning.

Cellular biochemical networks are highly interconnected: a perturbation in reaction rates or molecular concentrations may affect numerous cellular processes. The complexity of biochemical networks raises the question of the stability of their functioning. One possibility is that to achieve an appropriate function, the reaction rate constants and the enzymatic concentrations of a network need to be chosen in a very precise manner, and any deviation from the ‘fine-tuned’ values will ruin the network’s performance. Another

possibility is that the key properties of biochemical networks are robust; that is, they are relatively insensitive to the precise values of biochemical parameters. Here we explore the issue of robustness of one of the simplest and best-known signal transduction networks: a biochemical network responsible for bacterial chemotaxis. Bacteria such as *Escherichia coli* are able to sense (temporal) gradients of chemical ligands in their vicinity². The movement of a swimming bacterium is composed of a series of ‘smooth runs’, interrupted by events of ‘tumbling’, in which a new direction for the next run is chosen randomly. By modifying the tumbling frequency, a bacterium is able to direct its motion either towards attractants or away from repellents. A well established feature of chemotaxis is its property of adaptation^{10,13-16}: the steady-state tumbling frequency in a homogeneous ligand environment is insensitive to the value of ligand concentration. This property allows bacteria to maintain their sensitivity to chemical gradients over a wide range of attractant or repellent concentrations.

The different proteins that are involved in chemotactic response have been characterized in great detail, and much is known about the interactions between them (Fig. 1a). In particular, the receptors that sense chemotactic ligands are reversibly methylated. Biochemical data indicate that methylation is responsible for the adaptation property: changes in methylation of the receptor can compensate for the effect of ligand on tumbling frequency. Theoretical models proposed in the past assumed that the biochemical parameters are fine-tuned to preserve the same steady-state behaviour at different ligand concentrations^{17,18}. We present an alternative picture in which adaptation is a robust property of the chemotaxis network and does not rely on the fine-tuning of parameters.

We have analysed a simple two-state model of the chemotaxis network closely related to the one proposed previously^{2,19}. The two-state model assumes that the receptor complex has two functional states: active and inactive. The active receptor complex shows a kinase activity: it phosphorylates the response regulator molecules,

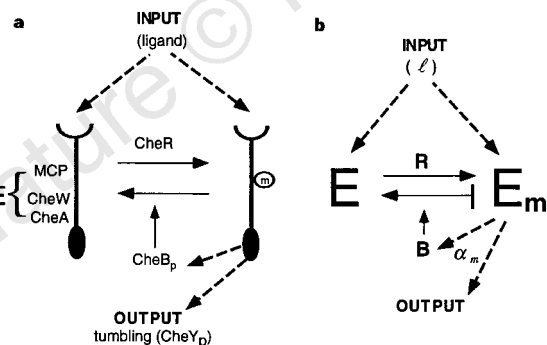


Figure 1 a, The chemotaxis network. Chemotactic ligands bind to specialized receptors (MCP) which form stable complexes (E), with the proteins CheA and CheW. CheA is a kinase that phosphorylates the response regulator, CheY, whose phosphorylated form (CheY_p) binds to the flagellar motor and generates tumbling. Binding of the ligand to the receptor modifies the tumbling frequency by changing the kinase activity of CheA. The receptor can also be reversibly methylated. Methylation enhances the kinases activity and mediates adaptation to changes in ligand concentration. Two proteins are involved in the adaptation process: CheR methylates the receptor, CheB demethylates it. A feedback mechanism is achieved through the CheA-mediated phosphorylation of CheB, which enhances its demethylation activity. **b**, Mechanism for robust adaptation. E is transformed to a modified form, E_m, by the enzyme R; enzyme B catalyses the reverse modification reaction. E_m is active with a probability of $\alpha_m(I)$, which depends on the input level I . Robust adaptation is achieved when R works at saturation and B acts only on the active form of E_m. Note that the rate of reverse modification is determined by the system’s output and does not depend directly on the concentration of E_m (vertical bar at the end of the arrow).

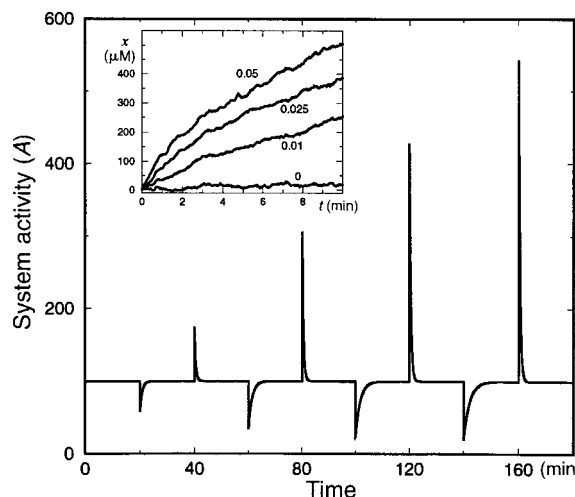


Figure 2 Chemotactic response and adaptation. The system activity, A , of a model system (the reference system described in Methods) which was subject to a series of step-like changes in the attractant concentration, is plotted as a function of time. Attractant was repeatedly added to the system and removed after 20 min, with successive concentration steps of I of 1, 3, 5 and 7 μM . Note the asymmetry to addition compared with removal of ligand, both in the response magnitude and the adaptation time. The chemotactic drift velocity of this system is presented in the inset. Inset: the different curves correspond to gradients $\nabla I = 0, 0.01, 0.025$ and $0.05 \mu\text{M}/\mu\text{m}$. An average change in receptor occupancy of less than 1% per second is sufficient to induce a mean drift velocity of the order of microns per second.

which then bind to the motors and induce tumbling. The receptor complexes can be either in the active or in the inactive state, although with probabilities that depend on both their methylation level and ligand occupancy. The average complex activity can be considered as the output of the network, whereas its input is the concentration of the ligand. A quantitative description of the model consists of a set of coupled differential equations describing interactions between protein components (Box 1).

The two-state model correctly reproduces the main features of bacterial chemotaxis. When a typical model system is subject to a step-like change in attractant concentration, l (Fig. 2), it is able to respond and to adapt to the imposed change. The adaptation is nearly perfect for all ligand concentrations. The addition (removal) of attractant causes a transient decrease (increase) in system activity, and thus of tumbling frequency. We observe a strong asymmetry in

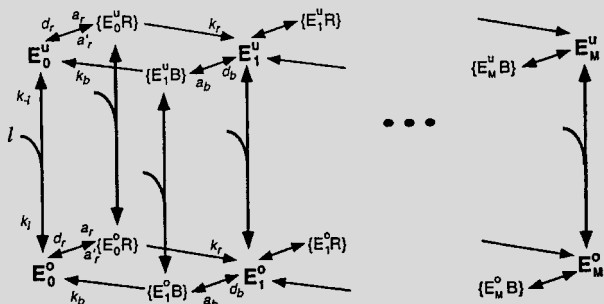
the response to the addition compared with the removal of ligand. This asymmetry has been observed experimentally¹⁴. The chemotactic response of the system has been measured by the average drift velocity in the presence of a linear gradient of attractant (Fig. 2, inset). The system is very sensitive: an average change in the receptor occupancy of $\sim 1\%$ per second is enough to induce a drift velocity of ~ 1 micron per second.

Figure 3a illustrates the most striking result of the model: we have found that the system shows almost perfect adaptation for a wide range of values of the network's biochemical parameters. Typically, one can change simultaneously each of the rate constants several-fold and still obtain, on average, only a few per cent deviation from perfect adaptation. For instance, over 80 per cent of model systems, obtained from a perfectly adaptive one by randomly changing all of its biochemical parameters by a factor of two, still show $<15\%$

Box 1 Two-state model of the bacterial chemotactic network

The main component of the two-state model^{2,19} is the receptor complex, MCP + CheA + CheW (Fig. 1a), considered here as a single entity, E. The complex is assumed to have two functional states—active and inactive. A receptor complex in the active state shows a kinase activity of CheA; by phosphorylating the response regulators, CheY, it sends a tumbling signal to the motors. The output of the network is thus the average number of receptors in the active state, the system activity A . It is assumed that this quantity determines the tumbling frequency of the bacteria. The transformation between A and the tumbling frequency depends on the kinetics of CheY phosphorylation and dephosphorylation, as well as on the interaction of CheY with the motors, which are not considered explicitly in the present model.

The receptor complexes are assumed to exist in different forms. Consider a complex methylated on m sites ($m = 1, \dots, M$). Such a complex can either be occupied or unoccupied by the ligand. We denote the concentration of these complexes by E_m^0 and E_m^u , respectively. Each form of the receptor complex can be in the active state with a probability depending on both its methylation level and its ligand occupancy. We assume that an occupied receptor complex has the probability α_m^0 of being in the active state; for an unoccupied receptor, this probability is α_m . If l is the ligand concentration, $B(R)$ the concentration of CheB (CheR), and $\{E_m^u B\}$ the concentration of the E_m^u CheB complex and so on, the model reactions can then be illustrated schematically (see figure).



The differential equations describing our model can be written in a standard way from the figure. For instance, the kinetic equation for E_m^u is

$$\frac{dE_m^u}{dt} = -k_f E_m^u + k_r E_m^0 + (1 - \delta_{m,0}) [-a_b \alpha_m E_m^u B + d_b \{E_m^u B\} + k_r \{E_{m-1}^u R\}] + (1 - \delta_{m,M}) [-a_r \alpha_m E_m^u R + a_i (1 - \alpha_m) E_m^u R + d_b \{E_m^u R\} + k_b \{E_{m+1}^u B\}]$$

$(m = 1, \dots, M)$

The presence of α_m in the equation is due the fact that CheB demethylates only the active receptors; we have also included two different association rate constants of CheR to the active (a_r) and the inactive (a_i) receptors (see below). δ_k is the Kronecker's delta ($\delta_k = 1$, when $j = k$, and is zero otherwise). Similar equations can be written to describe kinetics of $\{E_m^u B\}$, $\{E_m^0 R\}$, E_m^0 , $\{E_m^0 B\}$ and $\{E_m^0 R\}$, with additional parameters α_m^0 defining the probabilities of E_m^0 to be in the active state. For fixed α_m and α_m^0 the biochemical parameters of this system include nine different rate constants ($k_f, k_r, a_r, a_i, d_r, k_r, a_b, d_b, k_b$) and three enzyme concentrations (total concentrations of CheR, CheB and receptor complexes).

The present model is by no means the only two-state model of the chemotactic network that exhibits robust adaptation and proper chemotactic response. Rather, it is one of the simplest variants that is consistent with the experimental data on the response and adaptation of wild-type *E. coli*. The main assumptions underlying this model are as follows.

- The input to the system is the ligand concentration; rapid binding (and unbinding) of the ligand to the receptor induces an immediate change in the activity of the complex. For simplicity, the binding affinity is assumed to be independent of the receptor's activity and its degree of methylation. This assumption can be relaxed without affecting the main conclusions of our model.
- The methylation and demethylation reaction occur on slower timescales. A central assumption is that CheB can only demethylate active receptors. In addition, the demethylation rate constants do not depend explicitly either on ligand occupancy or on the methylation of the receptor, so that all active receptors are demethylated at the same rate. In the variant of the model discussed here, the phosphorylation of CheB is not considered explicitly; in molecular terms, we assume that the phosphorylated form of CheB, CheB_p, does not move freely in the cell. Rather, a CheB_p molecule can only demethylate the same receptor that has phosphorylated it. We note, however, that this assumption can also be readily relaxed (N.B. *et al.*, manuscript in preparation). Robust adaptation is maintained as long as both CheB and CheB_p demethylate only the active receptors.
- The methylating enzyme, CheR, acts both on active and inactive receptors. Here we assume that the association rate constant for this reaction depends only on the activity of the receptor (a_i for inactive, a_r for active), whereas the dissociation rate constant d_r and the catalytic rate constant k_r are the same for all forms of the receptor. This assumption can again be relaxed in various ways. In particular, the accumulated biochemical data indicate that CheR works at saturation and operates at its maximal velocity. In this case, the conclusions of our model are not altered, even if d_r, a_i and a_r depend on the ligand occupancy and on the methylation level²¹. □

deviation from perfect adaptation (Fig. 3a, lower panel). When varied separately, most of the rate constants may be changed by several orders of magnitude without inducing a significant deviation from perfect adaptation.

In our model we have assumed Michaelis–Menten kinetics for simplicity. However, we have found that cooperative effects in the enzymatic reactions can be added without destroying the robustness of adaptation. Similarly, robust adaptation is obtained for systems with different numbers of methylation sites. Multiple methylation sites are thus not required for robust adaptation, but possibly are for allowing strong initial responses for a wide range of attractant and repellent stimuli (N.B. *et al.*, manuscript in preparation).

The adaptation itself, as measured by its precision (Fig. 3a), is thus a robust property of the chemotactic network. This does not mean, however, that all the properties are equally insensitive to variations in the network parameters. For instance, Fig. 3b shows that the adaptation time, τ , which characterizes the dynamics of relaxation to the steady-state activity, displays substantial variations in the altered systems. Robustness is thus a characteristic of specific network properties and not of the network as a whole: whereas some properties are robust, others can show sensitivity to changes in the network parameters.

Plots similar to the ones depicted in Fig. 3 can be obtained in quantitative experiments. A large collection of chemotactic mutants can be analysed for variations in the biochemical rate constants of the chemotactic network components. Alternatively, the rate constants of the enzymes could be systematically modified or their expression varied. At the same time, their various physiological characteristics can be measured, such as steady-state tumbling frequency, precision of adaptation, adaption time, and so on. In this way, the predictions of the model can be quantitatively checked.

What features of the chemotactic network make the adaptation property so robust? We propose here a general and simple mechanism for robust adaptation. Let us introduce this mechanism for one of the simplest networks (Fig. 1b), which can be viewed either as an ‘adaptation module’, or, as a simplifying reduction of a more complex adaptive network, such as the one presented for bacterial chemotaxis. Consider an enzyme, E, which is sensitive to an external signal l , such as a ligand. Each enzyme molecule is at equilibrium between two functional states: an active state, in which it catalyses a reaction, and an inactive state, in which it does not. The signal level l affects the equilibrium between two functional states of the enzyme: we suppose that a change in l causes a rapid response of the system by shifting this equilibrium. Thus, l is the input of this signal transduction system and the concentration of active enzymes (that is, the system activity, A) can be considered as its output. The enzyme E can be reversibly modified, for example by addition of methyl or phosphate groups. The modification of E affects the probabilities of the active and inactive states, and hence can compensate for the effect of the ligand. In general, then, $A(l) = \alpha(l)E + \alpha_m(l)E_m$, where E_m and E are the concentrations of the modified and unmodified enzyme, respectively, and $\alpha_m(l)$ and $\alpha(l)$ are the probabilities that the modified and unmodified enzyme is active. After an initial rapid response of the system to a change in the input level, l , slower changes in the system activity proceed according to the kinetics of enzyme modification.

The system is adaptive when its steady-state activity, A^{st} , is independent of l . A mechanism for adaptation can be readily obtained by assuming a fine-tuned dependence of the biochemical parameters on the signal level, l . This kind of mechanism has been proposed for an equivalent receptor system^{17,18}. A mechanism for robust adaptation, on the other hand, can be obtained when the rates of the modification and the reverse-modification reactions depend solely on the system activity, A , and not explicitly on the concentrations E_m and E . This system can be viewed as a feed-back system, in which the output A determines the rates of modification

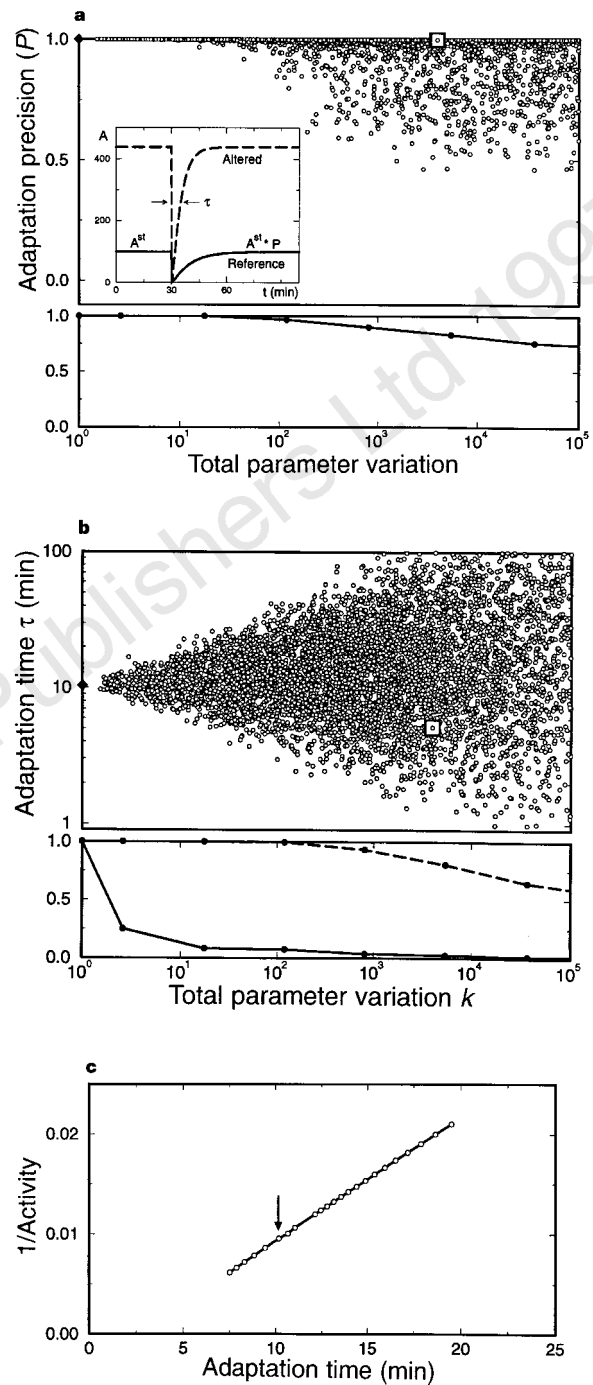


Figure 3 Robustness of adaptation. **a**, The precision of adaptation, P , and **b**, adaptation time, τ , to a step-like addition of saturating amount of attractant are plotted as a function of the total parameter variation k , for an ensemble of model systems (see Methods). The time evolution of the system activity A is depicted in the inset for the reference system (solid curve) and for an altered model system, obtained by randomly increasing or decreasing by a factor of two all biochemical parameters of the reference system (dashed curve). Each point in the top graphs in **a** and **b** corresponds to a different altered system, out of the total number of 6,157. The reference system is denoted by a black diamond; the particular altered system from the inset is denoted by an open square. Bottom graphs: **a**, the probability that P is larger than 0.95; **b**, the probability that τ deviates from the adaptation time of the reference system (~ 10 min) by less than 5% (solid curve) and by a factor 5 (dashed curve). **c**, ‘Individuality’ in the chemotaxis model. The inverse steady-state activity A^{-1} is plotted as a function of the adaptation time, τ . Each point represents an altered system, obtained from the reference system (arrow) by varying the concentration of CheR (between 100 to 300 molecules per cell).

reactions, which in turn determine the slow changes in A . With such activity-dependent kinetics, the value of the steady-state activity, A^{st} , is independent of the ligand level, therefore the system is adaptive. Activity-dependent kinetics can be achieved in a variety of ways. As a simple example, consider a system for which only the modified enzyme can be active ($\alpha = 0$); the enzyme R , which catalyses the modification reaction $E \rightarrow E_m$, works at saturation, and the enzyme B , which catalyses the reverse-modification reaction $E_m \rightarrow E$, can only bind to active enzymes. In this case, the modification rate is constant at all times, whereas the reverse modification rate is a simple function of the activity

$$\frac{dE_m}{dt} = V_{\text{max}}^R - V_{\text{max}}^B \frac{A}{K_b + A} \quad (1)$$

where V_{max}^B and V_{max}^R are the maximal velocities of the modification and the reverse-modification reactions, respectively, and K_b is the Michaelis constant for the reverse modification reaction; we have assumed $V_{\text{max}}^R < V_{\text{max}}^B$. For simplicity, we have assumed that the enzymes follow Michaelis–Menten (quasi-steady-state) kinetics. The functioning of the feedback can now be analysed: the system activity is continuously compared to a reference steady-state value

$$A^{\text{st}} = K_b \frac{V_{\text{max}}^R}{V_{\text{max}}^B - V_{\text{max}}^R}.$$

For $A < A^{\text{st}}$, the amount of modification increases, leading to an increase in A ; for $A > A^{\text{st}}$, the modification decreases, leading to a decrease in A . In this way, the system always returns to its steady-state value of activity, exhibiting adaptation. Moreover, with these activity-dependent kinetics, the adaptation properties is insensitive to the values of system parameters (such as enzyme concentrations), so adaptation is robust.

Note, however, that the steady-state activity itself, which is not a robust property of the network, depends on the enzyme concentrations. Thus, the mechanism presented here still provides a way to control the system activity on long timescales, for example by changing the expression level of the modifying enzymes while preserving adaptation itself on shorter timescales.

A quantitative analysis demonstrates that, on methylation timescales, the kinetics of the two-state model of chemotaxis can, for a wide range of parameters, be mathematically ‘reduced’ to the simple activity-dependent kinetics shown in equation (1) (N.B. *et al.*, manuscript in preparation). Robust adaptation thus follows naturally as consequence of the simple mechanism described above. The deviations from perfect adaptation (Fig. 3) are in fact connected to departures from the assumptions underlying this mechanism (such as $V_{\text{max}}^R < V_{\text{max}}^B$). This simple mechanism suggests that the various detailed assumptions about the system’s biochemistry can be easily altered, provided that the activity-dependent kinetics of receptor modifications is preserved. All variants of the model obtained in this way still exhibit robust adaptation (N.B. *et al.*, manuscript in preparation).

Two main observations argue in favour of a robust, rather than a fine-tuned, adaptation mechanism for chemotaxis. First, the adaptation property is observed in a large variety of chemotactic bacterial populations. It is easier to imagine how a robust mechanism allows bacteria to tolerate genetic polymorphism, which may change the network’s biochemical parameters. In addition, in genetically identical bacteria some features of the chemotactic response, such as the values of adaptation time and of steady-state tumbling frequency, vary significantly from one bacterium to another, while the adaptation property itself is preserved²⁰. This ‘individuality’ can be readily explained in the framework of the present model. The concentrations of some cellular proteins, for example the methylating enzyme CheR, are very low², and thus may

be subject to considerable stochastic variations. In consequence, both adaptation time and steady-state tumbling frequency, which are not robust properties of the network, should vary significantly. Moreover, the present model predicts that both these quantities should show a strong correlation in their variation (Fig. 3c), which has been observed experimentally²⁰.

How general are the results presented here? In addition to explaining response and adaptation in chemotaxis, the present model accounts, in a unifying way, for other taxis behaviour of bacteria mediated by the same network. Indeed, as the network’s dynamics is solely determined by the system activity, the system will respond and adapt to any environmental change that affects this activity. Mechanisms of robust adaptation similar to the one introduced above could apply to a wider class of signal transduction networks. Robustness may be a common feature of many key cellular properties and could be crucial for the reliable performance of many biochemical networks. Robust properties of a network will be preserved even if its components are modified through random mutations, or are produced in modified quantities. Systems whose key properties are robust could have an important advantage in having a larger parameter space in which to evolve and to adjust to environmental changes.

The degree of robustness in many biochemical networks can be quantitatively investigated. This can be achieved by characterizing a behavioural, a physical or biochemical property while varying systematically the expression level and the rate constants of the network’s components.

The complexity of biological systems introduce several conceptual and practical difficulties, however. Among the most important is the difficulty of isolating smaller subsystems that could be analysed separately. For instance, in the present analysis, we have neglected the existence of different types of receptors and any crosstalk between them. We have also disregarded the interactions between the chemotaxis network and other components of the cell. In addition, the complexity and stochastic variability of biological networks may preclude their complete molecular description. Rate constants and concentrations of many enzymes can only be measured outside their natural cellular environment and many other network parameters remain unknown. Robustness may provide a way out of both these quandaries: robust properties do not depend on the exact values of the network’s biochemical parameters and should be relatively insensitive to the influence of the other subsystems. It should then be possible to extract some of the principles underlying cell function without a full knowledge of the molecular detail. □

Methods

Numerical integration of the kinetics equations defining the two-state model (see Box 1) was used to investigate its properties. Computer programs in C++ language were executed on an SGI (R4000) workstation using a standard routine (*lsode* from LLNL). Typical CPU time for finding a numerical solution of a model system is of the order of 1 min. A particular model system was obtained by assigning values to the rate constants and the total enzyme concentrations. Most of our results were obtained for a reference system defined by the following biochemical parameters: the equilibrium binding constant of ligand to receptor is $1 \mu\text{M}$ and the time constant for the reaction is 1 ms ($k_1 = 1 \text{ ms}^{-1} \mu\text{M}^{-1}$, $k_{-1} = 1 \text{ ms}^{-1}$). CheR methylates both active and inactive receptors at the same rate, with a Michaelis constant of $1.25 \mu\text{M}$, and a time constant of 10 s ($a_r = a'_r = 80 \text{ s}^{-1} \mu\text{M}^{-1}$, $d_r = 100 \text{ s}^{-1}$, $k_r = 0.1 \text{ s}^{-1}$), CheB (CheB_p) demethylates only active receptors with a Michaelis constant of $1.25 \mu\text{M}$ and a time constant of 10 s ($a_b = 800 \text{ s}^{-1} \mu\text{M}^{-1}$, $d_b = 1,000 \text{ s}^{-1}$, $k_b = 0.1 \text{ s}^{-1}$). The number of enzyme molecules per cell are: 10,000 receptor complexes, 2,000 CheB and 200 CheR (cell volume of $1.4 \times 10^{-15} \text{ l}$). The probabilities that a receptor with $m = 1, \dots, 4$ methylated sites is in its active state are: $\alpha_1 = 0.1$, $\alpha_2 = 0.5$, $\alpha_3 = 0.75$, $\alpha_4 = 1$ if it is unoccupied, and $\alpha_1^0 = 0$, $\alpha_2^0 = 0.1$, $\alpha_3^0 = 0.5$, $\alpha_4^0 = 1$ if it is occupied.

Response and adaptation. In a typical assay, a model system was subject to a step-like change in attractant concentration. A system in steady-state, characterized by the system activity A^{st} , was perturbed by an addition or removal of attractant. As a result, the system activity changed abruptly and then relaxed, with the characteristic adaptation time, τ , to a new steady-state value $A^{st} \cdot p$. Here p measures the precision of adaptation; perfect adaptation corresponds to $p = 1$ (see inset in Fig. 3a).

Robustness of adaptation. The sensitivity of adaptation precision and adaptation time to variations in the biochemical constants defining a model system was investigated. An ensemble of altered systems was obtained from the reference system by random modifications of its reaction rate constants and enzymatic concentrations, k_n^0 . Each alternation of the reference system was characterized by the total parameter variation, k , which is defined as: $\log(k) = \sum_{n=1}^L |\log(k_n/k_n^0)|$, where k_n are the biochemical parameters of the altered system. The altered system was subject to a step-like addition of saturating concentrations of attractant (1 mM), and both the precision of adaptation, p , and the adaptation time, τ , were measured. The assay was repeated for various reference model systems, with different values of biochemical parameters and of α_m , and different variants of the model. The robustness of adaptation (Fig. 3) is independent of these choices.

Chemotactic drift velocity. The behaviour of a model system in the presence of a linear gradient of attractant, ∇l , was simulated. The movement of the system was assumed to be composed of a series of smooth runs at a constant velocity of $20 \mu\text{m s}^{-1}$, interrupted by tumbling events. The tumbling frequency was taken to be a sigmoidal function of the system activity (Hill coefficient, $q = 2$). Different values of q lead to the same qualitative picture; the sensitivity increases with q . The trajectories were also subject to a rotation diffusion, with $D = 0.125 \text{ rad}^2 \text{ s}^{-1}$ (ref. 9). Attractant concentration was increasing along the x direction, (with $l = 1 \mu\text{M}$ at $x = 0$). The chemotactic drift velocity was estimated by measuring the average x position of a hundred identical simulated systems as a function of time.

Received 31 December 1996; accepted 17 April 1997.

1. Bray, D. Protein molecules as computational elements in living cells. *Nature* **376**, 307–312 (1995).
2. Stock, J. B. & Surette, M. in *E. coli and S. typhimurium: Cellular and Molecular Biology* (ed. Neidhardt, F. C.) 1103–1129 (American Society of Microbiology, Washington DC, 1996).
3. Parkinson, J. S. Signal transduction schemes of bacteria. *Cell* **73**, 857–871 (1993).
4. Hazelbauer, G. L., Berg, H. C. & Matsumura, P. M. Bacterial motility and signal transduction. *Cell* **73**, 15–22 (1993).
5. Bourret, R. B., Borkovich, K. A. & Simon, M. I. Signal transduction pathways involving protein phosphorylation in prokaryotes. *Annu. Rev. Biochem.* **60**, 401–441 (1991).
6. Adler, J. Chemotaxis in bacteria. *Annu. Rev. Biochem.* **44**, 341–356 (1975).
7. Bray, D., Bourret, R. B. & Simon, M. I. Computer simulation of the phosphorylation cascade controlling bacterial chemotaxis. *Mol. Biol. Cell* **4**, 469–482 (1993).
8. Adler, J. Chemotaxis in bacteria. *Science* **153**, 708–716 (1996).
9. Berg, H. C. & Brown, D. A. Chemotaxis in *E. coli* analysed by three-dimensional tracking. *Nature* **239**, 500–504 (1972).
10. Macnab, R. M. & Koshland, D. E. The gradient-sensing mechanism in bacterial chemotaxis. *Proc. Natl Acad. Sci. USA* **69**, 2509–2512 (1972).
11. Block, S. M., Segall, J. E. & Berg, H. C. Impulse responses in bacterial chemotaxis. *Cell* **31**, 215–226 (1982).
12. Koshland, D. E. A response regulator model in a simple sensory system. *Science* **196**, 1055 (1977).
13. Berg, H. C. & Tedesco, P. M. Transient response to chemotactic stimuli in *E. coli*. *Proc. Natl Acad. Sci. USA* **72**, 3235–3239 (1975).
14. Springer, M. S., Goy, M. F. & Adler, J. Protein methylation in behavioural control mechanism and in signal transduction. *Nature* **280**, 279–284 (1979).
15. Koshland, D. E., Goldbeter, A. & Stock, J. B. Amplification and adaptation in regulatory and sensory systems. *Science* **217**, 220–225 (1982).
16. Khan, S., Spudich, J. L., McCray, J. A. & Tentham, D. R. Chemotactic signal integration in bacteria. *Proc. Natl Acad. Sci. USA* **92**, 9757–9761 (1995).
17. Segel, L. A., Goldbeter, A., Devreotes, P. N. & Knox, B. E. A mechanism for exact sensory adaptation based on receptor modification. *J. Theor. Biol.* **120**, 151–179 (1986).
18. Hauri, D. C. & Ross, J. A model of excitation and adaptation in bacterial chemotaxis. *Biophys. J.* **68**, 708–722 (1995).
19. Asakura, S. & Honda, H. Two-state model for bacterial chemoreceptor proteins. *J. Mol. Biol.* **176**, 349–367 (1984).
20. Spudich, J. L. & Koshland, D. E. Non-genetic individuality: chance in the single cell. *Nature* **262**, 467–471 (1976).
21. Kleene, S. J., Hobson, A. C. & Adler, J. Attractants and repellents influence methylation and demethylation of methyl-accepting proteins in an extract of *E. coli*. *Proc. Natl Acad. Sci. USA* **76**, 6309–6313 (1979).

Acknowledgements. We thank J. Stock, M. Surette, A. C. Maggs, U. Alon, L. Hartwell, M. Kirschner, A. Levine, A. Libchaber, A. Murray and T. Surrey for discussion; A. C. Maggs for help with numerical issues; and J. Stock, M. Surette and H. Berg for introducing us to bacterial chemotaxis and pointing out many useful references. This work has been partially supported by grants from the NIH and the NSF. N.B. is a Rothschild Fellow and a Dicke Fellow at Princeton University.

Correspondence and requests for materials should be addressed to S.L. (e-mail: leibler@princeton.edu).

A family of cytokine-inducible inhibitors of signalling

Robyn Starr*, Tracy A. Willson*, Elizabeth M. Viney*, Leeclia J. L. Murray*, John R. Rayner†, Brendan J. Jenkins†, Thomas J. Gonda†, Warren S. Alexander*, Donald Metcalf*, Nicos A. Nicola* & Douglas J. Hilton*

* The Walter and Eliza Hall Institute for Medical Research and The Cooperative Research Center for Cellular Growth Factors, Parkville, Victoria, Australia 3052

† The Hanson Centre for Cancer Research, IMVS, Adelaide, Southern Australia, Australia 5000

Cytokines are secreted proteins that regulate important cellular responses such as proliferation and differentiation¹. Key events in cytokine signal transduction are well defined: cytokines induce receptor aggregation, leading to activation of members of the JAK family of cytoplasmic tyrosine kinases. In turn, members of the STAT family of transcription factors are phosphorylated, dimerize and increase the transcription of genes with STAT recognition sites in their promoters^{1–4}. Less is known of how cytokine signal transduction is switched off. We have cloned a complementary DNA encoding a protein SOCS-1, containing an SH2-domain, by its ability to inhibit the macrophage differentiation of M1 cells in response to interleukin-6. Expression of SOCS-1 inhibited both interleukin-6-induced receptor phosphorylation and STAT activation. We have also cloned two relatives of SOCS-1, named SOCS-2 and SOCS-3, which together with the previously described CIS (ref. 5) form a new family of proteins. Transcription of all four SOCS genes is increased rapidly in response to interleukin-6, *in vitro* and *in vivo*, suggesting they may act in a classic negative feedback loop to regulate cytokine signal transduction.

To identify cDNAs encoding proteins capable of suppressing cytokine signal transduction, we used an expression cloning approach. The strategy used the murine monocytic leukaemic M1 cell line that differentiates into mature macrophages and ceases proliferation in response to various cytokines, including interleukin-6 (IL-6), and in response to the steroid, dexamethasone^{6,7}. Parental M1 cells were infected with the RUFneo retrovirus, into which a library of cDNAs from the factor-dependent haemopoietic cell line FDC-P1 had been inserted⁸. Retrovirally infected M1 cells that were unresponsive to IL-6 were selected in semi-solid agar culture by their ability to generate compact colonies in the presence of IL-6 and geneticin. One stable IL-6-unresponsive clone, 4A2, was obtained after examining 10⁴ infected cells (Fig. 1). A 1.4 kilobase pair (kbp) cDNA insert, which we have named suppressor of cytokine signalling-1, or SOCS-1, was recovered by polymerase chain reaction (PCR) from the retrovirus that had integrated into genomic DNA of 4A2 cells. The SOCS-1 PCR product was used to

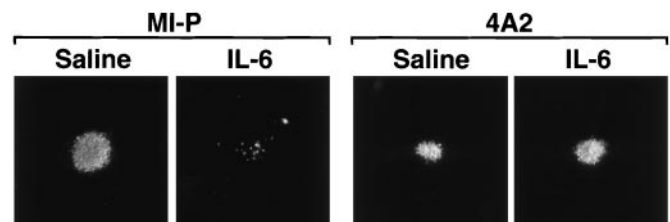


Figure 1 Phenotype of IL-6 unresponsive M1 cell clone, 4A2. Colonies of parental M1 cells (left panel) and clone 4A2 (right panel) cultured in semi-solid agar for 7 days in saline or 100 ng ml⁻¹ IL-6.